GYROTROPY AND ANISOTROPY OF ROCKS: SIMILARITIES AND DIFFERENCES

T. I. CHICHININA and I. R. OBOLENTSEVA

Institute of Geophysics of Russian Academy of Sciences (Siberian Branch)[1]

GYROTROPIE ET ANISOTROPIE DES ROCHES : SIMILITUDES ET DIFFÉRENCES

Les principales caractéristiques de la propagation des ondes dans les milieux gyrotropes sont comparées avec la propagation des ondes dans les milieux azimutalement anisotropes. Les résultats d'une modélisation numérique sont présentés pour trois modèles caractéristiques d'exploration sismique. Les deux premiers modèles sont des milieux anisotropes (de symétrie orthorhombique, groupe 2m) avec et sans gyrotropie. Le troisième modèle est un milieu gyrotrope transverse isotrope avec un axe de symétrie vertical. Ces calculs ont été réalisés pour la propagation des ondes transversales le long de l'axe de symétrie vertical. Pour des trajets sismiques suffisamment courts (pour nos modèles, moins de 400 m), les sismogrammes à deux composantes (x, y) sont similaires pour les trois modèles. Pour des trajets plus longs, la forme et la durée du signal diffèrent sensiblement pour les modèles 1 et 3.

Ceci a pour but de montrer (à l'aide des données expérimentales et d'un micromodèle) que la gyrotropie dans les roches existe, ou, tout au moins, peut exister.

GYROTROPY AND ANISOTROPY OF ROCKS: SIMILARITIES AND DIFFERENCES

The main features of wave propagation in gyrotropic media are compared with wave propagation in anisotropic media. The results of numerical modelling are presented for three typical seismic exploration models. The first two models are azimuthally anisotropic media (of orthorombic symmetry system, group 2m) without and with gyration. The third model is a gyrotropic transversely isotropic medium with a vertical symmetry axis. The computations have been made for propagation of shear waves along the vertical symmetry axis. For sufficiently short wave paths (in our models less than 400 m) the two-component (x, y) seismograms are similar for all three models. For longer paths both signal shape and signal duration for the first and the third model differ noticeably.

Some evidence (experimental data and a micromodel) is given to show that the gyrotropy of rocks does exist or, at least, can exist.

GIROTROPÍA Y ANISOTROPÍA DE LAS ROCAS : SEMEJANZAS Y DIFERENCIAS

Las principales características de la propagación de ondas en los medios girotrópicos se comparan con la propagación de ondas en medios anisotrópicos. Los resultados de la construcción de modelos numéricos se presentan a partir de tres modelos típicos

(1) Academician Koptug pr., 3, Novosibirsk, 630090 - Russia

de exploración sísmica. Los dos primeros modelos son medios azimutalmente anisotrópicos (de sistemas de simetría ortorrómbica, grupo 2m), sin y con giro. El tercer modelo es un medio girotrópico transversalmente isotrópico con un eje de simetría vertical. Los cálculos han sido hechos para la propagación de ondas de cizallamiento a lo largo del eje de simetría vertical. Para trayectos de onda suficientemente cortos (en nuestro modelo, menos de 400 m), los dos sismogramas componentes (x, y) son similares en los tres modelos. Para trayectorias más largas, tanto la forma de la señal como su duración difieren notablemente entre el primero y el tercer modelo.

Se entregan algunas evidencias (datos experimentales y un micromodelo) para mostrar que existe, o que al menos puede existir, la girotropía de las rocas.

INTRODUCTION

The polarization of shear waves is now a common tool in seismic prospecting for cracked hydrocarbon reservoirs. While in isotropic media the velocity of shear wave V_s is independent of polarization, in anisotropic media there are two shear waves (S_1, S_2) with mutually perpendicular polarization and generally different velocity. Azimuthal anisotropy of at least of monoclinic symmetry is caused by vertically oriented cracks. In such media one displacement vector $\boldsymbol{u}_{s_1}$ lies in the symmetry plane (parallel to the cracks) and the other displacement vector $\boldsymbol{u}_{s_2}$ is normal to this plane. If there are two systems of mutually perpendicular vertical cracks, the medium is orthorhombic and the displacement vectors lie in the two symmetry planes. For general acquisition geometries (i.e., the source-receiver direction does not coincide with the normal to a plane of symmetry or with one of the two normals if they are two), each of the three components (x, y, z) is the superposition of S_1 and S_2 waves propagating with velocities V_{s_1} and V_{s_2}. In this paper, we show that a similar two-component seismogram may correspond to a gyrotropic wave propagation.

The concept of seismic gyrotropy has recently been introduced [12-15]. Here we present briefly the main features of elastic wave propagation in an anisotropic gyrotropic geological medium and compare them with the features of wave propagation in purely anisotropic media.

1 ON PHENOMENOLOGICAL THEORY OF GYROTROPY

Optical gyrotropy (see, for example, [9, 5, 8 and 7]) is known since 1811 when F. Arago observed a rotation of the polarization plane of light propagating along an optical axis of quartz. By now the publications on optical gyrotropy run into the hundreds, and the optical gyrotropy is a powerful instrument in studying the fine structure of matter in many fields, e.g., physics of crystals, stereochemistry, biophysics, and biochemistry. Acoustical gyrotropy [1, 19-21, 4 and 23], the analog of optical gyrotropy, has been investigated much later, since the sixties of our century; the first were, to our knowledge, [1, 21, 19 and 20] and some others ([24, 25 and 6]), see [10]. Up to this point, the publications in acoustic gyrotropy are not as numerous as they are in optical gyrotropy. Nevertheless, the phenomenon

attracts much attention and is interesting both from the physical viewpoint and for its practical application.

Seismic gyrotropy can be regarded [12-15] as an extension of acoustic gyrotropy to geological media. Practically all the features of shear-wave polarizations observed in many seismic field experiments can be explained by a combination of two concepts: anisotropy and gyrotropy.

For electromagnetic and acoustic waves, gyrotropy of crystals is known as an exhibition of first-order spatial dispersion, i.e., non-local response of a crystal to a wave. Non-locality implies that in material equations $\mathbf{D} = E\,\mathbf{E}$, $\sigma = C\varepsilon$ that relate the electric displacement **D** to the electric field **E** and the stress σ to the strain ε, respectively, **D** and σ at a given point depend, respectively, on the **E** and ε not only at that point, but at neighbouring points as well. This dependence is expressed as a functional dependence $E(\omega, \boldsymbol{k})$ for electromagnetic waves and $C(\omega, \boldsymbol{k})$ for the acoustical analog. Here ω is circular frequency, and $\boldsymbol{k}$ is the wave vector of a plane harmonic wave with wave normal $\boldsymbol{n}$ and phase velocity V ($\boldsymbol{k} = \omega\,\boldsymbol{n}/V$). The above functions $E(\omega, \boldsymbol{k})$ and $C(\omega, \boldsymbol{k})$, are general in the sense that they account for both time frequency and spatial dispersion.

For seismic waves, we also accept, by analogy with acoustic waves, that $C = C(\omega, \boldsymbol{k})$. This assumption has been verified by numerous experimental data on polarizations of shear waves. As for causes of gyrotropy on a microlevel, one concrete micromodel of rock imitating sandy deposits of dissymmetric microstructure will be demonstrated below.

If the magnitude of the non-local part of the elastic stiffness C is small, the stiffness may be expanded in a power series in $\boldsymbol{k}$:

$$C_{ijkl}(w, \boldsymbol{k}) = c_{ijkl}(w) + ib_{ijklm}(w)\,k_m + d_{ijklmn}(w)\,k_m k_n + \ldots \quad (1)$$

In further considerations, we shall truncate this expansion after the second term:

$$C_{ijkl}(\omega, \boldsymbol{k}) = c_{ijkl}(\omega) + ib_{ijklm}(\omega)k_m \quad (2)$$

$\boldsymbol{c} = (c_{ijkl})$ is the well known tensor of elastic stiffnesses and $\boldsymbol{b} = (b_{ijklm})$ is the gyration tensor. The fifth rank tensor $\boldsymbol{b} = (b_{ijklm})$ is invariant relative to the rotation group and, hence, is not equal to zero only in acentric groups of symmetry. Its inner symmetry is:

$$b_{ijklm} = b_{jiklm} = b_{ijlkm} = b_{jilkm} = b_{ijklm} = -\,b_{klijm}$$

whereas the inner symmetry of the tensor $\boldsymbol{c}$ is:

$$c_{ijkl} = c_{jikl} = c_{ijlk} = c_{jilk} \text{ and } c_{ijkl} = c_{klij}$$

The dispersive term $ib_{ijklm}(\omega)\,k_m$ in Eq. (2) describes the effects which are called gyrotropy.

Hooke's law in a gyrotropic medium is:

$$\sigma_{ij} = c_{ijkl}\,\varepsilon_{kl} + b_{ijklm}\,\frac{\partial \varepsilon_{kl}}{\partial x_n} \quad (3)$$

where $\varepsilon_{kl} = (1/2)\,(\partial u_k/\partial x_i + \partial u_l/\partial x_k)$. The equations of motion $\partial\sigma_{ij}/\partial x_j = \rho\partial^2 u_l/\partial t^2$ become:

$$c_{ijkl}\,\frac{\partial^2 u_k}{\partial x_j \partial x_l} + b_{ijklm}\,\frac{\partial^3 u_k}{\partial x_j \partial x_l \partial x_m} = \rho\,\frac{\partial^2 u_i}{\partial t^2},\ i = 1,2,3. \quad (4)$$

For plane waves $\boldsymbol{u}(\boldsymbol{r}, t) = u_0\,\boldsymbol{A}\exp[i\omega(\boldsymbol{nr}/V - t)]$ propagating with phase velocity V in the direction of the wave normal $\boldsymbol{n}$ and polarized along a unit vector $\boldsymbol{A}$, Equations (4) are:

$$\left[c_{ijkl}n_j n_l + i\omega V^{-1} b_{ijklm} n_j n_l n_m\right] A_k = \rho V^2 A_i,\ i = 1,2,3 \quad (5)$$

or

$$\left[\Lambda_{ik} + \Delta_{ik} - V^2\delta_{ik}\right] A_k = 0,\ k = 1,2,3, \quad (6)$$

where $\Lambda_{ik} = c_{ijkl}\,\rho^{-1}\,n_j n_l$, ($\Delta_{ik} = i\omega\,V^{-1}\,\rho^{-1}\,b_{ijklm}\,n_j n_i n_m$).

The Equation (6) is the Christoffel equations for an anisotropic gyrotropic medium, and the tensor $(\Lambda + \Delta)$ is the appropriate Christoffel tensor.

The Equation (6) is a system of uniform equations which has non-trivial solution if its determinant is equal to zero:

$$\det\left(\Lambda_{ik} + \Delta_{ik} - V^2\delta_{ik}\right) = 0 \quad (7)$$

The determinant $\det(\Lambda_{ik} + \Delta_{ik} - V^2\delta_{ik}) = 0$ is a polynomial of the third degree in V^2 if the terms $\Lambda_{ik}\Delta^2{}_{kl}$ are disregarded. Equation (7) has three (positive) roots, the eigenvalues of the matrix. Then the solution of Equation (6) are three vectors $\boldsymbol{A}$ for three values (three eigenvalues and three eigenvectors of the matrix $(\Lambda_{ik} + \Delta_{ik} - V^2\delta_{ik})$, i.e., there are three waves as in an anisotropic medium without gyration). With the terms $\Lambda_{ik}\Delta^2{}_{kl}$ included, we have a polynomial of the fourth degree, and hence four solutions V^2_r, $\boldsymbol{A}_r$ ($r = 1,\ldots,4$) satisfy the system of Equation (6); four waves may be considered as a solution of Equation (4). However, the

parameters of the fourth wave are influenced also by the terms $d_{ijklmn}k_k k_l k_m k_n$ in the series expansion of Equation (1), which were omitted at the very beginning of our consideration.

The analysis of three-wave solution of Equation (4) shows that one wave is quasi-longitudinal (*qP*), and the other two waves are quasi-transverse (qS_1, qS_2). The phase velocities of all three waves slightly differ from the velocities in the medium without gyration (***b*** = 0). The main distinction from propagation in non-gyrotropic media is in polarizations which are no longer linear but elliptical. The ellipticity for *qP* wave is small, but for the two *qS* waves it can be large enough to be noticeable and result in significant consequences. Such a consequence is a rotation of the plane of shear-wave polarization due to right and left handed circular polarizations of waves qS_1, qS_2 having velocities $V_{s_1} = V_0 + \delta$ and $V_{s_2} = V_0 - \delta$, $\delta << V_0$. This phenomenon occurs in media of symmetry group $\infty\,\infty$ for all directions of propagation and along acoustic axes of threefold or higher symmetry in other acentric symmetry groups.

2 THE MAIN FEATURES OF GYROTROPIC PROPAGATION (NUMERICAL MODELLING)

To illustrate the main characteristics of shear waves in gyrotropic media, numerical modelling was performed. Since our main purpose is in providing examples of seismograms similar to those for non-gyrotropic but azimuthally anisotropic media, the following models have been chosen (Fig. 1). The first two models have orthorhombic symmetry, i.e., they are azimuthally anisotropic; model 1 is without gyration (it may be of any group symmetry within orthorhombic system), and model 2 is a gyrotropic one (it belongs to acentric group symmetry 2m). The stiffness tensors for both models are the same. The model 3 is transversely isotropic gyrotropic with a vertical symmetry axis.

Propagation along the vertical symmetry axis has been studied in all three models (Fig. 1). The source is situated inside the ground at the depth 2.4 km, and ten two-component receivers (*x*, *y*) are positioned above the source along a vertical profile at distances from *r* = 0.4 km to *r* = 2.2 km. The vector of the force in the source is in the *y*-direction of the *xyz* coordinate system. The directions of axes of this coordinate system are connected with the observation system and have been chosen arbitrarily.

In the models 1 and 2 the *x*-axis of the coordinate system *xyz* makes an angle $\psi = 30°$ with the X_1-axis of the system connected to the orthorhombic medium. The other two axes (X_2, X_3) of the crystallophysic coordinate system $X_1 X_2 X_3$ of the medium are oriented as follows: the X_3-axis is vertical, i.e., it coincides with the *z*-axis, and the X_2-axis makes the angle $\psi = 30°$ with the *y*-axis of the system *xyz*; both coordinate systems *xyz* and $X_1X_2X_3$ are right handed (Fig. 1).

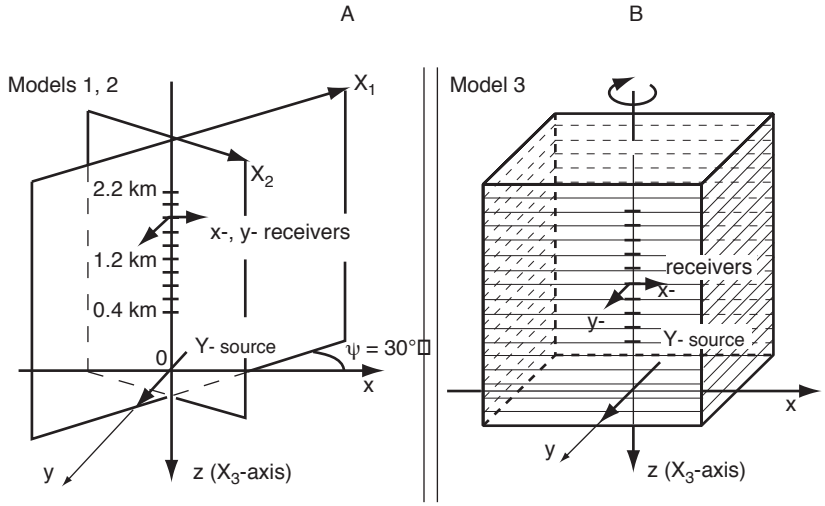

Figure 1

Models 1-3: A - orthorhombic medium model 1: non-gyrotropic, model 2: gyrotropic; B - gyrotropic transversely isotropic medium with a vertical symmetry axis.

In model 3 the symmetry axis X_3 of the transversely isotropic gyrotropic medium is directed along *z*-axis. The direction X_3 is an axial one, it controls the directions of circulation in two quasi-transverse waves (clockwise in the first- fast-wave and counter-clockwise in the second- slow-wave or vice versa).

The elastic and gyration constants for models 1-3 are given in Table 1 (in the coordinate system $X_1X_2X_3$). The stiffness matrix $\boldsymbol{c}$ is related to the tensor $\boldsymbol{c}$ in the usual manner. To characterize gyrotropy, the symmetrized gyration tensor and its dual, the fourth rank pseudo-tensor $\boldsymbol{g}$ are used. The tensor $\boldsymbol{g}$ and the symmetrized

TABLE 1

Matrices of elastic and gyration constants
($c_{ij}\,\rho^{-1}$, $g_{ij}\,\rho^{-1}\,km^2s^{-2}$)

Model 1

Matrix of elastic constants

9.747	1.775	2.377	0.0	0.0	0.0
1.775	5.957	2.347	0.0	0.0	0.0
2.377	2.347	7.491	0.0	0.0	0.0
0.0	0.0	0.0	2.007	0.0	0.0
0.0	0.0	0.0	0.0	2.437	0.0
0.0	0.0	0.0	0.0	0.0	2.386

Model 2

Matrix of elastic constants

9.747	1.775	2.377	0.0	0.0	0.0
1.775	5.957	2.347	0.0	0.0	0.0
2.377	2.347	7.491	0.0	0.0	0.0
0.0	0.0	0.0	2.007	0.0	0.0
0.0	0.0	0.0	0.0	2.437	0.0
0.0	0.0	0.0	0.0	0.0	2.386

Matrix of gyration constants

0.15	0.00	0.00	0.24	0.00	0.00	0.18	0.00	0.00	0.00
0.00	0.16	0.00	0.00	0.23	0.00	0.00	0.19	0.00	0.00
0.00	0.00	0.17	0.00	0.00	0.25	0.00	0.00	0.20	0.00

Model 3

Matrix of elastic constants

7.737	3.137	2.697	0.0	0.0	0.0
3.137	7.737	2.697	0.0	0.0	0.0
2.697	2.697	7.491	0.0	0.0	0.0
0.0	0.0	0.0	2.217	0.0	0.0
0.0	0.0	0.0	0.0	2.217	0.0
0.0	0.0	0.0	0.0	0.0	2.300

Matrix of gyration constants

0.03	0.00	0.00	0.01	0.00	0.00	0.02	0.00	0.00	0.00
0.00	0.03	0.00	0.00	0.02	0.00	0.00	0.01	0.00	0.00
0.00	0.00	0.02	0.00	0.00	0.04	0.00	0.00	0.03	0.00

gyration tensor b are related to each other by formulae: $g_{silm} = \omega/(2V)\ \delta_{sjk} b_{ijklm}$, $\omega/(V)\ b_{ijklm} = \delta_{jks} g_{silm}$ [23 and 12], where δ_{sjk} is the Levi-Civita symbol. The inner symmetry of the symmetrized tensor $\boldsymbol{b}$ differs from that of the tensor $\boldsymbol{b}$: the symmetrized tensor is antisymmetric in the permutation of the second and third indices and is symmetric in the permutation of the remaining three indices. The tensor $\boldsymbol{g}$ is symmetric in the permutation of the second, third and fourth indices and has 30 independent components [23]. The gyration constant matrix $\boldsymbol{g}$ is related to the tensor $\boldsymbol{g}$ as follows:

$$g_{1111}\ g_{1222}\ g_{1333}\ g_{1122}\ \ g_{1233}\ \ g_{1311}\ \ g_{1133}\ \ g_{1211}\ \ g_{1322}\ g_{1123}$$

$$g_{2111}\ g_{2222}\ g_{2333}\ g_{2122}\ \ g_{2233}\ \ g_{2311}\ \ g_{2133}\ \ g_{2211}\ \ g_{2322}\ g_{2123}$$

$$g_{3111}\ g_{3222}\ g_{3333}\ g_{3122}\ \ g_{3233}\ \ g_{3311}\ \ g_{3133}\ \ g_{3211}\ \ g_{3322}\ g_{3123}$$

Seismograms were computed by the ray method using algorithms and programs described in [17]. The two-component seismograms (Yx,Yy) are shown in Figure 2. The force direction in the source is Y (along the y-axis in Fig. 1) as it was mentioned above. The impulse in the source is a symmetric impulse $F(t) = \exp(-\beta t^2) \cos \omega t$ where $\beta = [\omega^2/(4\pi^2)] \ln R$ depends on R—ratio of the greatest, central, maximum to the nearest one; R is equal to 2.5, and the impulse is taken 2.5 periods long; f = 20 Hz.

2.1 The Seismogram for Orthorhombic Symmetry Medium (Model 1)

The y, x traces (Yy, Yx) are the superpositions of the two shear waves S_1, S_2 propagating along the symmetry axis z (X_3) with different ray velocities V_{s_1}, V_{s_2} and polarizations. Since along symmetry axes ray velocities are equal to phase velocities, the symbol V is used in the following for ray velocities though above it was used for phase velocities. The displacements in the fast wave, S_1, are in X_1-direction, and in the slow wave, S_2, they are in X_2-direction. The arrivals of S_2-wave are marked on the records with short vertical lines. One can see that at the receiver 1 (r = 0.4 km) the S_2-wave is later than S_1-wave by half of a period; in the middle of the receiver set, at the receiver 5 (r = 1.2 km), the time difference reaches two periods, and for the last receiver 10 (r = 2.2 km) the waves S_1, S_2 are fully separated because the time difference becomes nearly 2.5 periods, i.e., it is a little greater then the duration of the impulse.

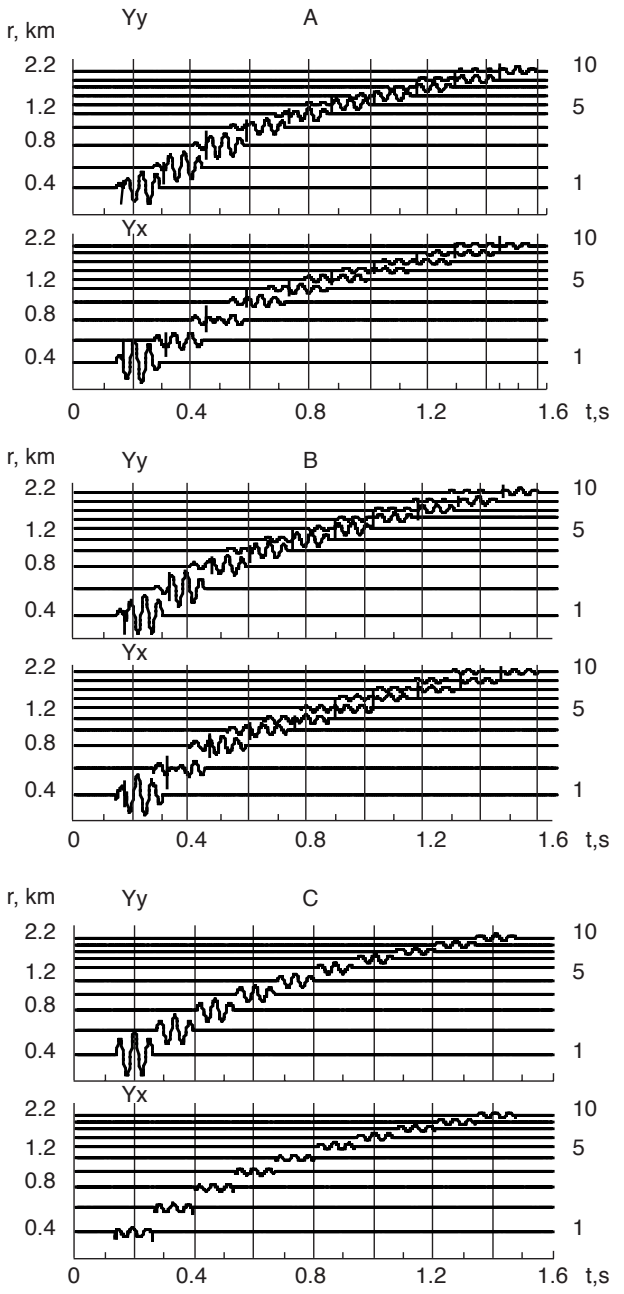

Figure 2

Two-component (Yy, Yx) seismograms of shear waves for propagation along the symmetry axes of media with parameters given in Table 1. A: non-gyrotropic orthorhombic medium (ψ = 30°); B: gyrotropic orthorhombic medium (ψ = 30°); C: gyrotropic transversely isotropic medium with vertical axis of symmetry.

2.2 The Seismogram for Orthorhombic Symmetry Gyrotropic Medium (Model 2)

The gyrotropy is expected to slightly change the velocities of shear waves S_1, S_2 propagating along the two-fold symmetry axis and to convert the linear polarizations into elliptical ones. The velocity of the fast wave S_1 slightly increases, and the velocity of the slow S_2-wave slightly decreases:

$$|\delta V_{s_1}| / V_{s_1} = 0.012, \quad |\delta V_{s_2}| / V_{s_2} = 0.015$$

The ellipticity (a ratio of small-axis length to large-axis length) is approximately equal to 0.35 for both waves.

The differences between the non-gyrotropic and gyrotropic propagation can be seen from the seismograms in Figure 2 (A) and (B). At first glance, it seems that the two seismograms are very similar. However, more careful correlation between the corresponding traces in Figure 2 (A) and (B) shows that the differences are consistent with the expectations.

Some records differ noticeably in pattern; see, for example, traces *Yx* with numbers 2, 3, 6, 7, 9, 10. These and other differences can be seen more distinctly in Figure 3 where the traces *Yy, Yx* for the nearest, the central and the most distant reception points are shown. The nearest records, at the distance r = 0.4 km, practically do not differ. The records at the distance r = 1.2 km are also rather similar with the exception of the short time interval after the first arrival of the second (slower) wave, particularly on the record *Yx*. At the greatest distance r = 2.2 km, the waves S_1, S_2 in the gyrotropic medium are very well separated ($\delta t \approx 1.2\,T$, where T is a visible period) whereas in the non-gyrotropic medium the separation is much less distinct ($\delta t \approx 0.3\,T$).

One more difference of records in Figure 2 (A) and (B) is that in (B) the signal lasts longer than in (A). The reason is in that in the gyrotropic medium the first wave arrives earlier and the second wave later than in the case of the same medium without gyration.

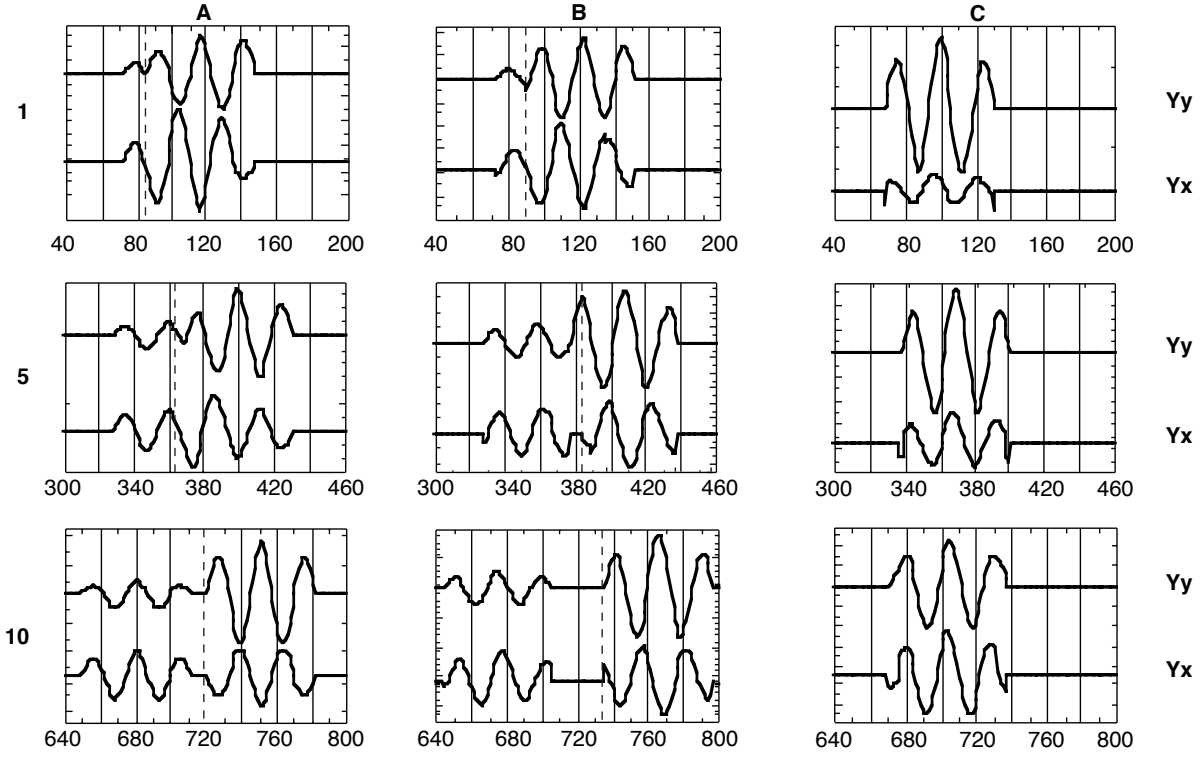

Figure 3

Traces numbers 1, 5, 10 of seismograms given in Figure 2: A - model 1, B - model 2, C - model 3.

2.3 The Seismogram for the Transversely Isotropic Gyrotropic Medium with Vertical Symmetry Axis (Model 3)

This model has been chosen to demonstrate the most interesting feature of gyrotropic propagation, the rotation of the plane of polarization of shear waves, i.e., a turn of displacement vector $\boldsymbol{u}_y$ (generated by *Y*-source) after passing through such a medium. The turn angle α can be determined from the ratio of amplitudes on *x* and *y* traces: $\alpha \approx \tan^{-1} u_x/u_y$. Exact equality holds for harmonic oscillations. If a wave is harmonic, the ratio u_x/u_y is:

$$u_x/u_y = \tan\frac{\varphi_1 - \varphi_2}{2} = \tan\frac{\omega r}{2}\left(\frac{1}{V_{S_1}} - \frac{1}{V_{S_2}}\right) \qquad (8)$$

where $(\varphi_1 - \varphi_2)$ is the phase difference of the two shear waves with circular right and left-handed polarizations, and $V_{s_1} = V_{s_0} - \delta$, $V_{s_2} = V_{s_0} + \delta$, are their velocities which are equal to the velocity V_{s_0} in the same medium without gyration by addition and subtraction, respectively, of the gyrotropic correction δ; *r* is a distance source-receiver.

In the model under consideration, the velocities of propagation of shear waves along *z*-axis are $V_{s_{1,2}} = V_{s_0} \pm \delta = 1.489 \pm 0.007\ \mathrm{km\,s^{-1}}$, the visible frequency $f = \omega/(2\pi) = 20$ Hz. Substituting these values in Equation (8) one obtains the following values of turn angle α:

$r = 0.4$ km (receiver 1) $\alpha = \tan^{-1} 0.1525 \approx 8.7°$;
$r = 1.2$ km (receiver 5) $\alpha = \tan^{-1} 0.4928 \approx 26.2°$;
$r = 2.2$ km (receiver 10) $\alpha = \tan^{-1} 1.0980 \approx 47.7°$.

Figure 2 (C) shows the increase of the ratio u_x/u_y from the receiver 1 to the receiver 10. This increase of *x*-component amplitude relatively to the *y*-component can be more clearly seen in Fig. 3 (C). The ratios u_x/u_y are approximately equal to those given above for a harmonic wave of frequency $f = 20$ Hz.

The main conclusion from the comparison of two-component (*x, y*) seismograms for models 1-3 is that they can be rather similar if the wave path is sufficiently short, in the considered case $r \leq 0.4$ km for frequencies of order 20 Hz and $V_s \approx 1.5\ \mathrm{km\,s^{-1}}$. However, *x,y*-patterns for orthorombic symmetry (model 1) depend on the azimuth of the horizontal axis (X_1) relative to the *x*-axis of the coordinate system of the observer. If a medium is transversely isotropic gyrotropic with a vertical X_3-axis (model 3), *x, y* seismograms are the same for all azimuths. The influence of gyrotropy on propagation along X_3 symmetry axis of a medium of orthorombic symmetry is recognizable with great difficulty. In real media, attenuation affects the propagation of two shear waves and changes the above described *x, y* -patterns.

3 SOME EVIDENCES OF SEISMIC GYROTROPY

3.1 Experimental Data

Seismic gyrotropy could have been observed already in the sixties in many experiments in which shear and converted *PS* waves were recorded on two (*x, y*) or three components (*x, y, z*) if the concept of seismic gyrotropy had then already existed. Two phenomena characterize seismic gyrotropy: turn of a displacement vector (rotation of polarization plane) and elliptical polarizations. The first phenomenon occurs only in gyrotropic media and therefore is easier detectable. The turn angle is in direct ratio to gyration constant, frequency, and path length and in inverse ratio to the cube of the shear wave velocity in the same medium without gyration:

$$\alpha = \frac{\pi f r D}{V_0^3} \qquad (9)$$

D is a quadratic gyrotropic addition to V_0^2 $(V_{s_{1,2}}^2 = V_0^2 \pm D)$, and $V_0 = (V_{s_1} + V_{s_2})/2$ [14 and 15]. Equation (9) can be brought into the form:

$$\alpha = \frac{\pi f r (D/V_0^2)}{V_0} \qquad (10)$$

with dimensionless parameter D/V_0^2.

Direct proportionality between turn angle α and frequency *f* was yet observed in 1976 by I.S. Chichinin [26]. The vibrator worked in a harmonic regime at the frequencies 20, 30, ..., 80 Hz. The displacement vector of a direct shear wave recorded in the borehole in alluvial deposits of Ural river at a depth of 83 m was rotating with increasing frequency. The plane of polarization turned in the whole by $\approx 50°$. Later the dependence α (*f*) was studied at borehole investigations for alluvial deposits of the river Ob (near Tomsk) and

its tributary Chulym (near Almyakovo) for depths 0-18 m [22, 12, 14]. The data are shown in Figure 4. As in the earlier experiment [26], the angle increases with increasing frequency, but not monotonously.

The dependence α (r) is shown in Figure 5. It was found in the above experiments, for the frequency f = 100 Hz. Rotation power, or specific rotation, is found to be $\approx 1 \div 1.5$°/m. This result is rather stable.

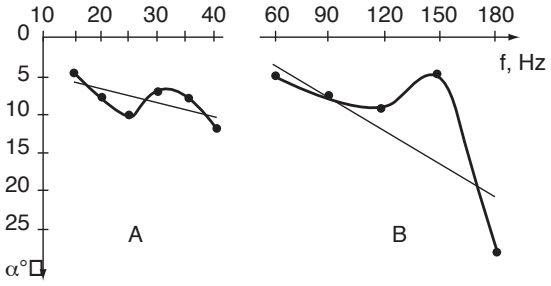

Figure 4

Dependence of turn angle α on frequency f for two frequency ranges: A, vibrator source; B, impulse source.

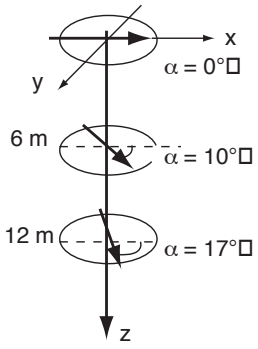

Figure 5

Dependence of turn angle α on distance r.

The values of gyration constant have also been determined. Since all real media are attenuative, one observed in experiments the rotation of an ellipse, not of a displacement vector (Fig. 6). The ellipse rotates by the same angle as the vector [12 and 14]. To take attenuation into account, one can write for velocities V_{s_1}, V_{s_2}:

$$V_{s_1} = V_0 + a - ib\,; \quad V_{s_2} = V_0 - a - ib \tag{11}$$

The attenuation coefficients of waves S_1, S_2 are functions of constants a, b introduced in (11):

$$\beta_1 = \frac{\omega b}{|V_{s_1}|^2}, \quad \beta_2 = \frac{\omega b}{|V_{s_2}|^2} \tag{12}$$

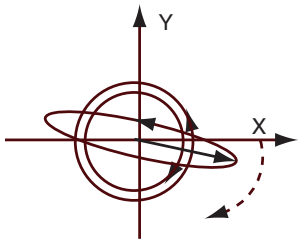

Figure 6

Ellipse as a sum of two circular oscillations of opposite directions with not equal amplitudes and velocities.

The gyration constant a and attenuation constant b are determined from the system of equations:

$$\frac{\exp(-\omega r b_1)}{\exp(-\omega r b_2)} = \frac{1 + B/A}{1 - B/A}, \quad \omega r (a_2 - a_1) = 2\alpha$$

where:

$$a_1 = (V_0 + a)/|V_{s_1}|^2, \quad a_2 = (V_0 - a)/|V_{s_2}|^2$$

$$b_1 = b/|V_{s_1}|^2, \qquad b_2 = b/|V_{s_2}|^2$$

If the ratio B/A of the axes of the ellipse and the orientation a of the major axis are known, one can find the constants. The following estimates of ratios a/V_0, b/V_0 have been found for the upper part of the ground (0-20 m) in the seismic frequency range (10-100 Hz) [22 and 14]:

$$a/V_0 \approx 0.03, \; b/V_0 \approx 0.35 \tag{13}$$

At geoacoustic frequencies (of order $\approx$ 500 Hz), the ratios a/V_0, b/V_0 for the same depth interval are [18]:

$$a/V_0 \approx 0.01, \; b/V_0 \approx 0.20 \tag{14}$$

Using refracted waves we could estimate the ratios a/V_0, b/V_0 for the depth interval 50-300 m in the frequency range 20-30 Hz. S_1 and S_2 waves exited by Y

and *Z* vibrator sources have been observed at the distances 260-1080 m. The experiments were performed near Chulym river near the site of the borehole investigations for studying gyrotropy in the uppermost of the underground. We found for depth interval ~ 50-200 m the following ratios [16]:

$$a/V_0 \approx 0.02,\ b/V_0 \approx 0.01 \qquad (15)$$

The data in Equations (13), (14) and (15) are consistent. The values of ratio b/V_0 lead to the realistic values of attenuation. In a gyrotropic medium, there are two attenuation coefficients β_1, β_2, see Equation (12). It was found in observations of refracted waves *SV*, *SH* that, due to gyration, $\beta_{SV} = 0.0046\ m^{-1}$, $\beta_{SH} = 0.0048\ m^{-1}$.

Thus, the shallow subsurface is characterized by the values $a/V_0 \approx 0.01$-0.03, $b/V_0 \approx 0.01$-0.35. Over the same depth range, the velocity changes from 150-250 m/s to 500 m/s. The rotation power is equal to ≈ 1-1.5°/m. For rocks at greater depths, the rotation power is expected to be less than for near-surface formations because it is in inverse ratio to cube of the velocity, if D = const (Eq. (9)), and inverse to the velocity V_0, if D/V_0^2 = const (Eq. (10)). Therefore, to compute seismograms for *S*-wave propagation along symmetry axis in a gyrotropic medium (model 3, Fig. 1B) for the depth interval 0.4 km-2.2 km, the elastic and gyration constants were taken as follows:

$$c_{33}\,\rho^{-1} = 2.217,\quad g_{3333}\,\rho^{-1} = 0.02\ (km^2 s^{-2}).$$

In this case, one has for the ratio a/V_0: $a/V_0 = 0.007/1.489 \approx 0.005$ and, hence, $D/V_0^2 \approx 0.010$; $V_0 = 1.489 km\ s^{-1}$. This yields a rotation power of 0.02°/m.

3.2 Model of grainy rocks of dissymmetric microstructure

3.2.1 Constructing the model

In describing this model, we follow the papers [3 and 2], where it is presented in more detail. The model considered here has first been suggested—together with two other gyrotropic models—in [15].

To construct a model of grainy rock possessing gyrotropic properties, we "spoil" a regular cubic packing of spheres in the following manner (Fig. 7): in each column centres of spheres are so displaced that their projections on a horizontal plane *XY* lie on an arc of a circle of radius *R*, all being displaced in one direction:

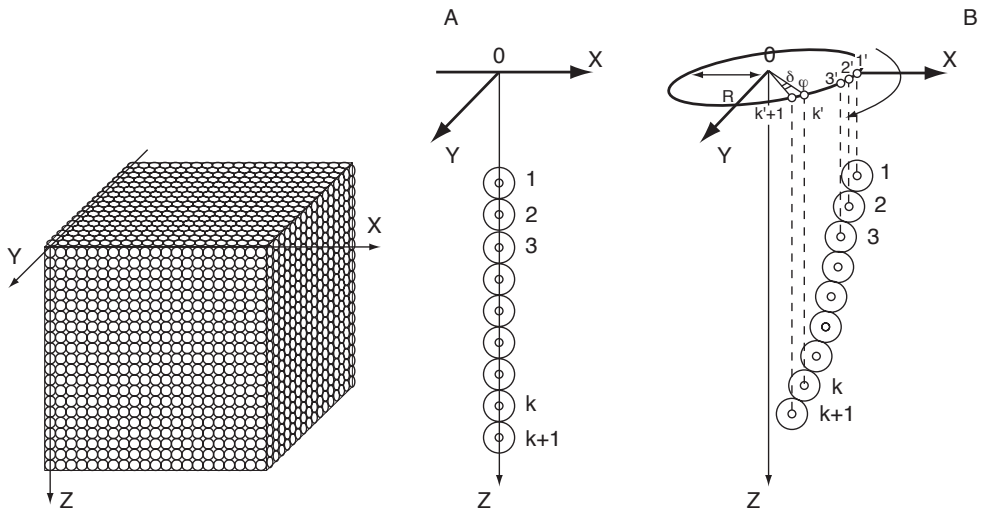

Figure 7

Constructing of the "grainy" medium with broken symmetry. A: a regular cubic packing of spheres and a column of spheres; B: a column of spheres in the disturbed packing of spheres and projections on *XY* plane of centres of spheres.

clockwise or counter-clockwise. The displacements of spheres ought to be very small with central angles of the order $\delta\varphi \approx 0.01\text{-}0.00001°$. This condition provides turn angles of shear-wave displacement vectors of the same order as in experiments which were briefly discussed in the previous subsection.

The dissymmetric model for collections of grains is obtained by translation the "spoilt" column in the *X*- and *Y*- directions. The introduced dissymmetry of the model leads to the same dissymmetry in positions for top and bottom contact points of spheres as it is shown in Figure 8.

The relative positions of contact points *T, B* on the grain surface can be characterized by the azimuthal angle $\delta\varphi$ and the polar angle θ. The angle $\angle\, T^*O^*B^*$ between the points T^* and B^*, projections of points *T, B* on a horizontal plane, is equal to $\pi\text{-}\delta\varphi$. The two parameters θ and $\delta\varphi$ are dissymmetry parameters for a grain of radius R_0.

The dissymmetric model is built on the principle of spiral, by analogy with the models in optics and acoustics (see, for example, micromodels of quartz and tellurium ([7 and 6]). The discrepancy is that the azimuthal angle $\delta\varphi$ is extremely small, and therefore a movement not along a spiral is imitated, but along a rather limited part of a spiral, namely along a part of a half-spire. In other words, it can be said that the dissymmetric model is built in accordance with the principle "an azimuthal turn plus translation".

3.2.2 Solution of Dirichlet problem inside a grain

The task is to clarify whether the spiral model rotates the polarization plane of a shear wave. A radius of a sphere is much less than a wavelength ($R_0 << \lambda$), therefore the problem of wave propagation can be reduced to the problem of a static equilibrium of a sphere, an element of the model.

Let the forces $\mathbf{Q}_1$, $\mathbf{Q}_2$, $|\mathbf{Q}_1|=|\mathbf{Q}_2|= Q$ be applied at the top (*T*) and the bottom (*B*) points of each sphere (Fig. 9), and let, for simplicity, these forces be radial. The forces $\mathbf{Q}_1$, $\mathbf{Q}_2$ have horizontal components, and therefore we have a possibility to model shear-wave propagation along *z*-axis.

The equilibrium equation for a sphere is:

$$\mathrm{div}\sigma_{ij} = (\lambda + \mu)\,\mathrm{grad\ div}\,\boldsymbol{u} + \mu\Delta\boldsymbol{u} = 0$$

where λ, μ are the Lame constants of the grain material. A solution of this equation inside the sphere was searched for in Papkovich form [11]. The algorithm has been built for computing displacement vectors, their first and second derivatives and components of stress tensor. It could be shown that in such a dissymmetric medium a displacement vector does turn. The means to determine gyrotropy constants for the constructed model was found and gyration constants have been computed [3, 15, 2]. The dependence of gyration constants on the dissymmetry parameters and grain material was also studied.

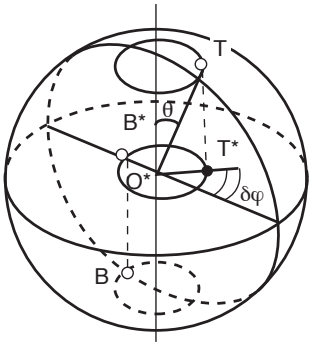

Figure 8

Top (*T*) and bottom (*B*) contact points on the surface of a sphere.

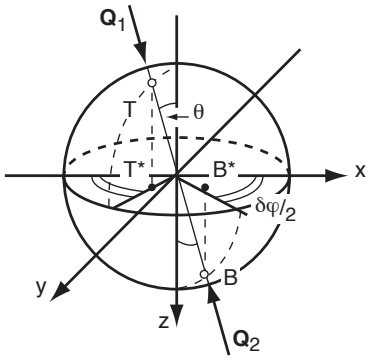

Figure 9

The forces $\mathbf{Q}_1$, $\mathbf{Q}_2$ applied to the grain surface at the points *T* and *B*; *xyz* is a local coordinate system connected with a grain.

3.2.3 Modelling of rotation of polarization plane

Consider modelling of *S*-wave propagation along the *Z*-axis, and let the wave be polarized originally (for $Z = 0$) in *Y*-direction so that $\mathbf{U} = |U|\boldsymbol{e}_2$, where **U** is a polarization vector of the wave. For the case considered, the rotation of the vector **U** means that it should acquire a *X*-component [12 and 14]. The tangent of the turn angle Φ of the polarization vector $\mathbf{U} = U_x \boldsymbol{e}_1 + U_y \boldsymbol{e}_2$ is determined by the ratio U_x/U_y: $\tan\Phi = U_x/U_y$.

Consider the "initial" grain (with a number $k = 1$) in the column of spheres of the dissymmetric model. The polarization vector **U** for the first grain (at $Z = 0$) is directed along *Y*-axis as it is shown in Figure 10.

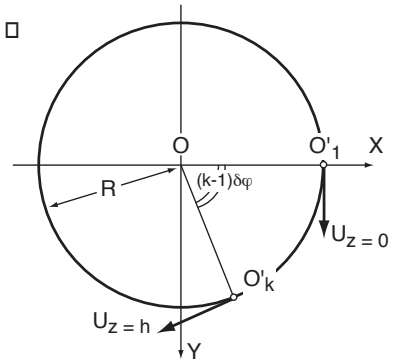

Figure 10

Polarization vector **U** for the first grain ($Z = 0$) and for the *k*-th grain ($Z = h$). O'_1 and O'_2 are projections of the grain centres on the circle of radius *R*.

The "abnormal" component of the displacement is not formed yet: $U_x = 0$, and the turn angle of the polarization vector is equal to zero: $\Phi = 0$. The vector **U** on the *k*-th grain (at $Z = h$) has got a *X*-component (Fig. 10), and the angle Φ became = $\Phi \tan^{-1} (U_x/U_y)$. The angle Φ increases monotonously in the wave propagation from grain to grain in the interval from $k = 0$ to $k = n$. All grains give the identical contribution to the total turn angle of the polarization vector **U**.

3.2.4 Results of calculations

For the dissymmetric model in Figure 9, the displacements u_x and u_y were computed. Parameters of the model are: radius of a grain $R_0 = 10^{-4}$ m, Lame constants $\mu = 10^8$ Nm^{-1}, $\lambda = 2\mu$, the applied force $Q = 10^{-2}$ N and the dissymmetry parameters $\theta = 10°$, $\delta\varphi = 0.06°$.

Calculations show that polarization vector turns by an angle 1° at the depth $Z = 0.8$ cm. Thus, to provide rotation power of shear-wave polarization plane equal 1° per metre, as it is observed in experiments, it is sufficient to have a thin gyrotropic layer, for this case, $h = 0.8$ cm (or fourty rows of grains 0.02 cm in diameter) in a layer of 1m thick. This means that, on the average, nearly every hundredth grain in the column should be displaced in the manner mentioned. As this takes place, the other grains may form a regular cubic packing or to be displaced in such a way that for each grain with dissymmetry parameter $\delta\varphi$ there will be a grain with $\delta\varphi + \pi$ for the summary turn be equal to zero.

The model must be dissymmetric in a statistical sense. The most correct approach is a probabilistic one. In this case, the dissymmetry parameters of the model are random values. The probability-density curve for the angle $\delta\varphi$ must be asymmetric relatively a value $\delta\varphi = 0$.

CONCLUSIONS

The comparison of gyrotropic and non-gyrotropic propagation of shear waves in media of interest for seismic prospecting offers a clearer view of how to distinguish gyrotropy and anisotropy. The distinction is most difficult when a shear wave passes through a layer of insufficient thickness. For a medium with $V_s = 1.5$ km/s and frequencies of about 20 Hz such difficulties can exist when layers are less than 200-400 m thick. This problem will be investigated in the near future.

ACKNOWLEDGMENTS

The work was supported by *Russian Fund of Fundamental Investigations (RFFI)* grant 97-05-16282.

REFERENCES

1 Andronov A.A. (1960) On natural rotation of polarization plane of sound. *Izv. Vuzov, Radiophys.*, III, 4, 645-649.

2 Chichinina T.I. (1998) Constructing of a grainy medium model possessing gyrotropic properties. *Geol. and Geoph.*, 7, 10, 1450-1465.

3 Chichinina T.I. and Obolentseva I.R. (1997) Gyrotropic properties of rocks due to a dissymmetry of microstructure. In: *Modern Practice in Stress and Vibration Analysis, Proceedings of the 3rd International Conference* held in Dublin, 3-5 September 1997, M.D. Gilchrist (Ed.), Balkema, Rotterdam, Brookfield, 425-430

4 DiVincenzo D.P. (1986) Dispersive corrections to continuum elastic theory in cubic crystals. *Phys. Rev*., B34, 8, 5450-5465.

5 Fedorov F.I. (1976) *Theory of Gyrotropy*, Minsk.

6 Hulin M. (1965) Lattice dynamics of tellurium, 1965. In: *Lattice Dynamics*, R.F. Wallis (Ed.), 135-140, Pergamon, Oxford.

7 Kizel V.A. and Burkov V.I. (1980) *Gyrotropy of Crystals*, Nauka, Moscow.

8 Konstantinova A.F., Grechushnikov B.N., Bokut B.V. and Valyashko E.G. (1995) *Optical properties of Crystals*, Navuka i tekhnika, Minsk.

9 Landau L.D. and Lifshits E.M. (1992) *Electrodynamics of Solids*, Nauka, Moscow.

10 *Lattice Dynamics* (1965) R.F. Wallis, (Ed). Pergamon, Oxford.

11 Lurie A.I. (1955) *Three-Dimensional Problems of Elasticity Theory*, Gostekhizdat, Moscow.

12 Obolentseva I.R. (1992) Seismic gyrotropy. In: *Investigations of Seismic Waves Propagation in Anisotropic Media*. I.S. Chichinin (Ed.) 6-45, Nauka, Novosibirsk.

13 Obolentseva I.R. (1993) On symmetry properties of the gyration tensor characterizing spatial dispersion of elastic media. In: *Elastic Waves in Gyrotropic and Anisotropic Media*, I.R. Obolentseva (Ed.), 5-23, Nauka, Novosibirsk.

14 Obolentseva I.R. (1996) On seismic gyrotropy. *Geophys. J. Int.*, 124, 415-426.

15 Obolentseva I.R. and Chichinina T.I. (1997) Seismic gyrotropy and its physical reasons. *Geol. and Geoph.*, 38, 5, 999-1013.

16 Obolentseva I.R. and Durynin A.F. (1993) Experimental study of gyrotropic properties of terrigeneous sediments using observations of shear refracted waves. In: *Elastic Waves in Gyrotropic and Anisotropic Media*. I.R. Obolentseva (Ed.), 95-127, Nauka, Novosibirsk.

17 Obolentseva I.R. and Grechka V.Yu. (1989) *Ray Method in Anisotropic Medium (algorithms, programs)*, Nauka, Novosibirsk.

18 Obolentseva I.R., Nefedkin Yu.A. and Krylov D.V. (1996) Determination of gyration and attenuation constants in sandy-clayey deposits of the upper part of the ground using borehole geoacoustic observations. *Inverse Problems of Geophysics, Proceedings of the International Workshop* held in Novosibirsk, September 30-October 4, Novosibirsk, 141-144.

19 Pine A.S. (1970) Direct observation of acoustic activity in α-quartz. *Phys. Rev*., B, 2, 2049-2054.

20 Pine A.S. (1971) Linear wave-vector dispersion of the shear-wave phase velocity in α-quartz. *J. Acoust. Soc. Am.*, 49, 1026-1029.

21 Portigal D.L. and Burstein E. (1968) Acoustical activity and other first-order spatial dispersion effects in crystals. *Phys. Rev.* 170, 3, 673-678.

22 Rezyapov G.I. (1992) Experimental investigation of the origin of anomalous polarization of shear waves propagating along the vertical in a low velocity zone. In: *Investigations of Seismic waves Propagation in Anisotropic Media*. I.S. Chichinin (Ed.) 104-111., Nauka, Novosibirsk.

23 Sirotin Yu.I. and Shascolskaya M.P. (1979) *Fundamentals of Crystallophysics*, Nauka, Moscow.

24 Toupin R.A. (1962) Elastic materials with couple-stresses. *Arch. Rational Mech.* Anal. 11, 5, 385-414.

25 Toupin R.A. and Gazis D.C. (1965) Surface effects and initial stress in continuum and lattice models of elastic crystals. *Lattice Dynamics*, In: R.F. Wallis (Ed.), Pergamon, Oxford, 597-605.

26 Vasilyev V.I., Evchatov G.P., Okuneva V.F. *et al.*, (1976) Experimental investigations of seismic waves excitation process by vibrator source. In: *Seismic Waves Excitation Problems by Vibrator Source*, IGiG SO AN SSSR, N.N. Puzyrev, I.S. Chichinin (Ed.) Novosibirsk, 65-86.

Final manuscript received in July 1998